scientific reports

Check for updates

OPEN

Human fetal lung mesenchymal stem cells ameliorate lung injury in an animal model

Mahtab Golmohammadi[1], Mohammad Hasan Sheikhha[1], Fatemeh Ganji[2], Ali Shirani[3], Mahmood Barati[4,5], Seyed Mehdi Kalantar[1], Seyed Mohammad Amin Haramshahi[4,6], Nushin Karkuki Osguei[7] & Ali Samadikuchaksaraei[5]✉

Acute lung injury (ALI) is a critical condition with limited treatment options. This study evaluates the therapeutic potential of human fetal lung-derived mesenchymal stem cells (hFL-MSCs) in an experimental model of ALI. Our proof-of-concept findings suggest a paradigm shift in the approach to cell sourcing for lung diseases, proposing that fetal lung cells may be potential targets for stem cell differentiation studies when the derived cells are intended to be used for lung cell therapy. After characterizing hFL-MSCs, 18-week fetal lung cells were intratracheally instilled into rats with bleomycin-induced ALI. All the animals were evaluated on days 3 – 28 post-injury for cell count and the cytokines in bronchoalveolar lavage fluid (BALF), lung wet/dry weight ratio, lung tissue histological staining and expression of an extracellular matrix component, inflammatory and fibrotic genes. The findings confirm mesenchymal stem cell identity of the isolated cells and stability in their cell cycle distribution. Analysis of BALF showed that immune cell response to acute inflammation and adaptive immunity was significantly ameliorated by cell therapy with hFL-MSCs. Same results were confirmed by the levels of IL-6, TNF-α, IL-10 and NO in BALF, the lung wet/dry weight ratio and histopathological analysis of lung tissues after H&E and Masson's trichrome staining. Effective modulation of key pro-inflammatory (*Il6*, *Tnf*, *Il1b*), pro-fibrotic (*Tgfb1*) and *Col1a1* genes were also confirmed after therapy with hFL-MSCs. Our findings suggest that fetal lung tissue-specific stem cells are viable options for lung cell therapy and could be considered as targets for engineering of regenerative cells for lung diseases.

Keywords Mesenchymal stem cells, Acute lung injury, Pulmonary fibrosis, fetal tissues, Cell therapy

Acute lung injury (ALI) involves widespread inflammation and increased lung vascular permeability, often leading to morbidity and mortality. Management remains supportive, with no specific treatments to reverse its pathology[1]. This highlights the need for novel strategies that can effectively target the complex pathophysiological mechanisms driving this condition.

Given the crucial role of alveolar type II (ATII) cells in lung injury repair[2], several studies were focused on using these cells[3] or ATII cells derived from stem cells[4–6] for cell therapy of lung injury. However, recent studies have increasingly focused on the potential of mesenchymal stem cells (MSCs) in treatment of ALI. The current evidence suggests that MSCs can be as effective as ATII cells in cell therapy of ALI[7]. Mesenchymal cells offer significant advantages for industrial-scale production due to their high potential for in vitro expansion on automated platforms. These systems enhance consistency, scalability, and safety, effectively addressing challenges such as maintaining cell quality and preventing contamination[8,9]. In contrast, epithelial cells (e.g. ATII cells) are less adaptable to such platforms.

The potential of MSCs in treatment of ALI has been highlighted in several studies[10–12] confirming their unique properties of anti-inflammatory[13], anti-fibrotic[14] and immunomodulatory effects[15]. In a recent study, pluripotent stem cell-derived MSCs were successfully employed for cell therapy in a mouse model of ALI[16].

[1]Department of Medical Genetics, Shahid Sadoughi University of Medical Sciences, Yazd, Iran. [2]Latner Research Laboratories, Division of Thoracic Surgery, University Health Network, Toronto, ON, Canada. [3]The Persian Gulf Biomedical Research Institute, Bushehr University of Medical Sciences, Bushehr, Iran. [4]Cellular and Molecular Research Centre, Iran University of Medical Sciences, Tehran, Iran. [5]Department of Medical Biotechnology, Faculty of Allied Medicine, Iran University of Medical Sciences, Tehran 1449614535, Iran. [6]Department of Tissue Engineering & Regenerative Medicine, Faculty of Advanced Technologies in Medicine, Iran University of Medical Sciences, Tehran, Iran. [7]Eposcience Millennium Institute, Tehran, Iran. ✉email: samadikuchaksaraei@yahoo.com; ali.samadi@iums.ac.ir

In this context, fetal lung-derived mesenchymal stem cells are of particular interest given their lung-specific properties[17]. Fetal cells exhibit significant plasticity and a high rate of proliferation[18], as well as a preference for homing to and regenerating their tissue of origin[19]. The latter, i.e. engraftment in the lung tissue, is critical for effective treatment of ALI[20,21].

Recent advances in stem cell biology have expanded our understanding of how different cell types can be harnessed for lung regeneration, particularly in the context of acute lung injury (ALI). As mentioned above, ATII cells have been traditionally considered the prime candidates for regenerating lung tissue. Consequently, our previous efforts focused on creating a versatile cell source for lung regeneration by differentiating pluripotent stem cells into ATII cells, ensuring that it could be readily generated on demand and in sufficient quantities[4,22,23]. However, based on the observations mentioned above, we hypothesized that fetal respiratory cells might be more viable targets for cell therapy in lung injury. To prove this concept, we have successfully studied the therapeutic potential of human fetal respiratory epithelial cells in an experimental model of lung injury[24]. In the current study, we extend these findings by demonstrating the therapeutic benefits of human fetal lung mesenchymal stem cells in the same disease model. Our results strongly support the notion that fetal lung-derived cells represent a promising cell source for the development of novel therapies for ALI and mark a paradigm shift in how we approach lung regeneration.

Materials and methods

All methods in this study were performed in accordance with the national guidelines set by the Iranian Ministry of Health. Also, the study is reported in accordance with ARRIVE guidelines.

Cell isolation and characterization from fetal lungs

Fetal lung tissues were collected from 20 cadaveric fetuses post-spontaneous abortion with written consent. The fetuses were aged from 12 to 19 weeks of gestation. The fetuses with disorders in their respiratory and cardiovascular systems and those from mothers having any infectious diseases or any hormonal and respiratory tract disorder were excluded from the study. Complete list of inclusion and exclusion criteria is presented in **Table S1** (Supplementary data). Mesenchymal cells were isolated from the lung tissues by dissociated cell culture and expanded under the standard conditions. The cells that achieved 80% of confluence and had passage numbers ranging from 3 to 7 were subjected to further studies. From 20 fetal lungs, we successfully cultured an adequate number of cells from a 16-week and an 18-week lung at passage numbers 3 to 7, which were used for this study. Cells from different fetuses were cultured separately and not pooled.

The isolated cells were examined by flow cytometry for expression of specific surface markers for mesenchymal stem cells (MSCs) and their functional potential was assessed by osteogenic and adipogenic differentiation. The details of these methods are presented in the supplementary Materials and Methods.

Cell cycle measurement

The passage 3 mesenchymal cells cultured in the medium described in Sect. "Induction of acute lung injury in rat" were harvested after two days. One million cells were fixed in 70% ethanol for 10 min at room temperature and treated with 0.5 µg/ml RNase. Then, they were stained with 5 µg/ml propidium iodide for 30 min at 37 °C. Finally, the DNA content was measured using flow cytometry (FACSCalibur, Becton Dickinson, USA).

Population doubling level

Population doubling level (PDL) of mesenchymal cells, derived from 16 and 18-week-old fetuses, were examined as described by Jahromi et al., 2015[25]. For this purpose, 1×10^5 cells were seeded per well of 6 well culture plates. Population doubling levels were determined after 24, 48, 72, and 168 h using the following formula:

$PDL = 3{:}32 \times (\log N_H - \log N_I)$ (1).

where N_H and N_I were the numbers of the harvested and inoculated cells at the given time points.

Animal study and cell therapy

Induction of acute lung injury in rat

The healing potential of human fetal lung mesenchymal stem cells (hFL-MSCs) was evaluated in the rat model of acute lung injury (ALI). Based on the assessment of population doubling levels (PDLs) in hFL-MSCs, cells derived from 18-week fetal lung were chosen for cell therapy. This decision was due to their significantly higher PDL compared to cells derived from 16-week fetuses, measured at 72 h and beyond. For this experiment, 36 male Sprague-Dawley rats, weighing 200–250 g (Pasteur Institute, Iran), were housed with free access to standard food pellets and tap water. As described before[24], ALI was induced by our established protocol using intratracheal instillation of 2.5 U/kg Bleomycin (Nippon Kayaku, Japan) under anesthesia with 80 mg/kg ketamine and 8 mg/kg xylazine hydrochloride (both from Alfasan Co, Netherlands). The rats were divided into the three experimental groups including Group 1, the control group receiving PBS instead of bleomycin and cell suspension (− BLM, $n = 12$); Group 2, the rats with induced ALI that did not undergo cell therapy, received PBS instead of cell suspension (+ BLM, $n = 12$); and Group 3, the rats with induced ALI that underwent cell therapy with passage 3 of hFL-MSCs derived from 18-week fetal lung at day 0 (BLM + MSC, $n = 12$). In Group 3, two hours after BLM instillation, the rats received a suspension of 3×10^6 hFL-MSCs in 200 µl of PBS by intratracheal instillation. The rats were scarified by lethal doses of ketamine and xylazine 3, 7, 14 and 28 days after the bleomycin instillation. Subsequently, bronchoalveolar lavage fluid (BALF) were collected from all groups and analyzed for cell count and cytokine measurement. Additionally, tissue samples were prepared for histological evaluation. Lung wet/dry weight ratio assay and gene expression analysis were also performed. Induction of ALI was confirmed by comparison of groups 1 and 2 for these variables, as described below.

Bronchoalveolar lavage fluid analysis

Bronchoalveolar lavage was performed with 3 ml of sterile PBS. BALF was collected and centrifuged at 1300 ×*g* for 10 min. The supernatant was isolated and frozen at − 70 °C for cytokine assessment and the cell pellet was re-suspended in PBS. Total and differential cell counts were determined on a grid hemocytometer.

IL-6, TNF-α and IL-10 levels were measured in the BALF supernatant using ELISA kits (R&D Systems, Minneapolis, USA) according to the manufacturer's instructions, and the absorbance was evaluated at 450 nm using a microplate reader (BioTek, ELx808 model, Winooski, VT, USA).

The level of nitric oxide in the BALF was determined by a colorimetric assay using Griess reagent as described before[26]. For this assay, equal volumes of BALF and Griess reagent (Sigma Aldrich, MO, USA) were mixed and the absorbance was measured at 540 nm using a microplate reader (Synergy HTX, Bio Tek, USA). A standard curve was plotted using sodium nitrite (Merck, Germany) to quantify NO levels.

Lung wet/dry weight ratio assay

This assay was employed as an index to evaluate the extent of lung edema. It measures the proportion of water content in lung tissue, reflecting the severity of edema following acute lung injury and subsequent cell therapy. At the end of each experiment, a 5 × 5 × 3 mm tissue block was excised from the right lung of each rat ($n = 3$) and weighed immediately to obtain the wet weight (W). All the samples were then reweighed after being freeze-dried at − 80 °C for 24 h to determine the dry weight (D). The W/D ratio was calculated using the following formula:

$$W/D\ ratio\ =\ \frac{Wet\ weight}{Dry\ weight} \tag{2}$$

This ratio provides an indication of the relative water content in the lung tissue.

Histological evaluations

On days 3, 7, 14, and 28 after bleomycin instillation, the lung tissues were harvested and fixed with formaldehyde. After routine H&E staining, the sections underwent a semiquantitative histopathologic scoring. Masson's trichrome staining was also performed to evaluate collagen deposition. The details of these protocols, including the statistical analysis methods, are presented in the supplementary Materials and Methods.

Real-time RT-PCR

Using Real-time RT-PCR, relative expression of the genes with pro-inflammatory (*Il6*, *Tnf*, *Il1b*) and pro-fibrotic (*Tgfb1*) functions and *Cola1* gene that expresses the extracellular matrix component collagen type 1, α1 chain were assessed in harvested lungs. The details are presented in the supplementary Materials and Methods.

Statistical analysis

Graph Pad Prism (Version 6.1, Graph Pad Software, CA, USA) was used for statistical analysis. Method of comparison was determined according to the results of Kolmogorov-Smirnov and F tests results. So, parametric comparison of means was performed by t-test and ANOVA (with Tukey's multiple comparisons test). The data are presented as mean ± standard deviation (SD). Mean differences at p values < 0.05 were considered statistically significant.

Results

Cell characterizations

Morphology and molecular markers

Mesenchymal cell isolated from the lungs of the 16- and 18-week-old fetuses exhibited a spindle-shaped morphology under phase-contrast microscopy (Fig. 1A). Additionally, flow cytometric analysis of isolated cells revealed that the levels of expression of mesenchymal stem cell markers CD73, CD90 and CD105 were greater than 95% (positive expression), while the expression levels of hematopoietic lineage markers CD34 and CD45, as well as the HLA-DR marker, were less than 2% (negative expression) (Fig. 1B and supplementary **Fig. S1 and Fig. S2**).

Osteogenic and adipogenic differentiation

Osteogenic differentiation was confirmed by staining for calcium deposition (Alizarin Red) and adipogenic differentiation was confirmed by detection of adipose droplets with Oil Red O staining (Fig. 1C). Although chondrogenic differentiation was not assessed in this study, the demonstrated osteogenic and adipogenic potential, together with the results of flow cytometric analysis, strongly supports the mesenchymal stem cell identity of the isolated cells.

Cell cycle measurement

The results of cell cycle distribution, as illustrated in Fig. 1D and supplementary **Fig. S3**, show that the distribution of cells across different cell cycle phases did not significantly differ between the two gestational ages. At both 16 and 18 weeks, the majority of the MSCs were in the G0/G1 phase, and the sub-G1 population, indicative of apoptotic cells, was minimal.

These findings indicate that the cell cycle characteristics of MSCs from the human fetal lung are stable between 16 and 18 weeks of gestation.

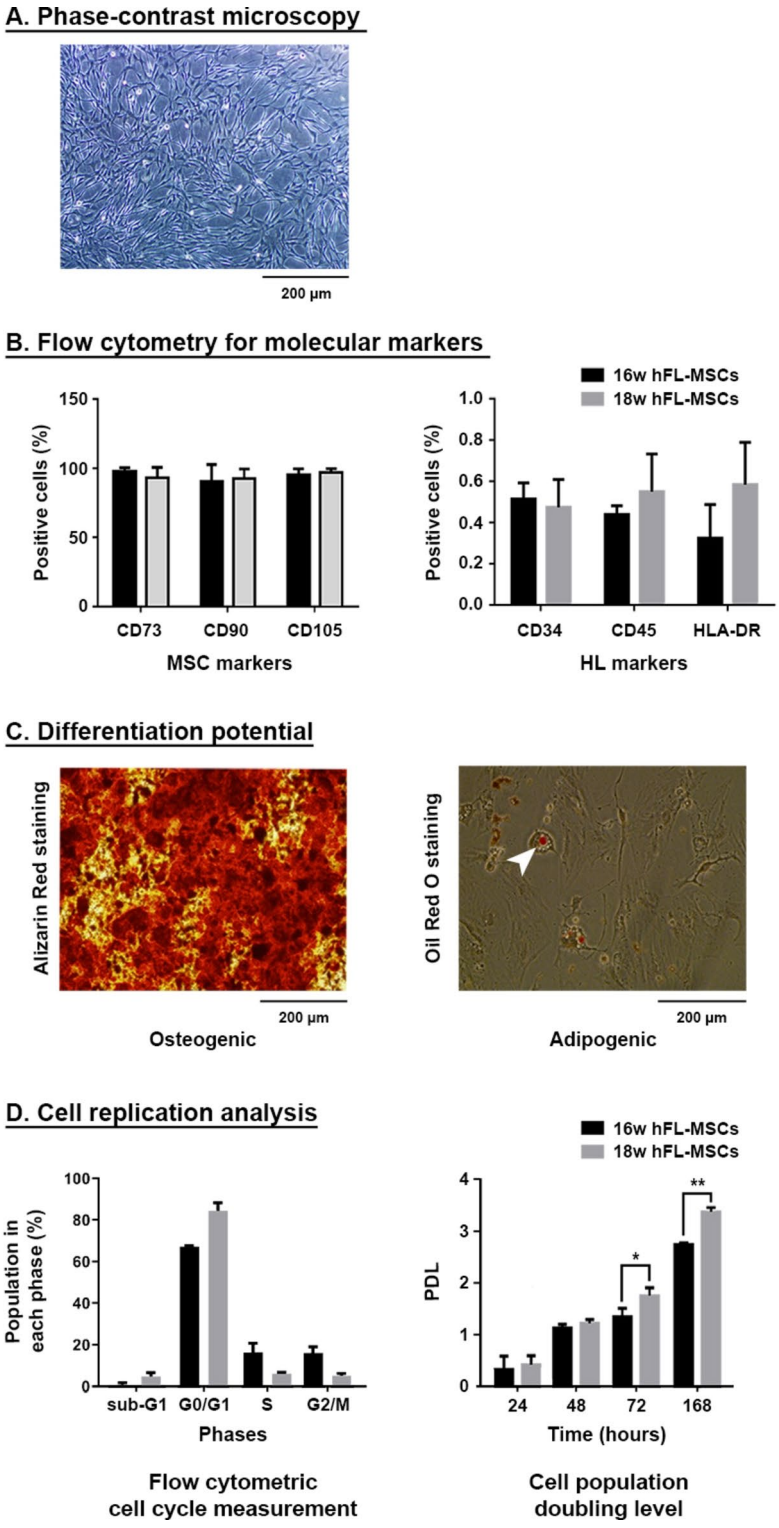

Population doubling level

Assessment of the population doubling level (PDL) of hFL-MSCs derived from 16 and 18-week-old fetuses (Fig. 1D) showed that there was no significant difference in PDL between the two groups at 24 and 48 h. However, at 72 h, the 18-week hFL-MSCs exhibited a significantly higher PDL compared to the 16-week cells ($p < 0.05$). This trend continued at 168 h, where the 18-week cells showed a marked increase in PDL ($p < 0.01$). Based on this finding, 18-week hFL-MSCs were selected for cell therapy in the animal model of ALI.

Animal study and cell therapy

Cell counts in BALF

Analysis of bronchoalveolar lavage fluid (BALF) samples (Fig. 2A) showed the highest count of total white blood cells (WBC) in the BLM-treated group that did not undergo cell therapy (+BLM). Whereas after cell therapy

◀**Fig. 1**. Cell characterization. (**A**) A representative phase-contrast microscopy of the mesenchymal cells isolated from human fetal lungs at both 16- and 18-week of gestation showing typical spindle-shaped morphology. (**B**) The results of flow cytometric identification of the cells expressing molecular markers of mesenchymal stem cells (> 95% expression; positive expression) and hematopoietic lineage (< 2% expression; negative expression); representative histograms are presented in supplementary **Fig. S1** and **Fig. S2**. (**C**) Representative photomicrographs showing functional capacity of isolated human fetal lung mesenchymal cells to differentiate into osteogenic (Alizarin Red staining) and adipogenic (Oil Red O staining) phenotypes. White arrowhead points to a red-stained lipid droplet. (**D**) Cell replication analysis of the mesenchymal cells isolated from 16- and 18-week human fetal lungs showing the results of flow cytometric measurement of the percent of the cells in each phase of cell cycle (representative histograms are presented in supplementary **Fig. S3**) and the population doubling levels of these cells. Abbreviations: 16w, 16-week; 18w, 18-week; hFL-MSCs, human fetal lung mesenchymal stem cells; PDL, population doubling level.
Data are mean ± SD; *$p < 0.05$, **$p < 0.01$ (Only statistically significant differences between groups are indicated in the figure).

(BLM + MSC group), total WBC count showed a significant decrease at all time points. The changes of the numbers of neutrophils, macrophages and lymphocytes after induction of the acute lung injury (+ BLM versus − BLM) shows an expected pattern of domination of innate immune response on days 3 and 7 and involvement of adaptive immune response on day 14. This is reflected by a significant increase in the number of neutrophils and macrophages up to day 14 and number of lymphocytes on day 14 after injury (+ BLM versus − BLM). The cell counts on day 28 show an expected transition from acute inflammation to a resolution and repair phase as + BLM group does not show elevated neutrophil and lymphocyte counts but, macrophage count is still elevated compared with − BLM group. These 28-day macrophages could be those with anti-inflammatory and reparative phenotype.

After cell therapy with hFL-MSCs (BLM + MSC group), our results show a significant decrease in the counts of neutrophils, macrophages, and lymphocytes at the same time points where these cells were elevated in the + BLM group compared to controls.

ELISA assay in BAL fluid samples

As expected, analysis of BALF in the + BLM group compared to controls (− BLM) (Fig. 2B) showed an early increase in the pro-inflammatory cytokines IL-6 (up to day 14) and TNF-α (up to day 7), correlating with the acute inflammatory phase. On the other hand, the anti-inflammatory cytokine IL-10 showed a transient rise on day 7, reflecting the activation of regulatory mechanisms to control inflammation. By day 28, the levels of these cytokines in the + BLM group were not significantly different from those in the − BLM group. This return to baseline levels is consistent with the resolution of acute inflammation and ongoing tissue repair.

Our findings indicate that after cell therapy with hFL-MSCs (BLM + MSC group), there was a significant decrease in the levels of all the cytokines at the same time points where these cytokines were elevated in the + BLM group compared to controls.

Nitric oxide (NO) assay in BAL fluid samples

In acute lung injury, the upregulation of NO production is typically driven by inflammatory cytokines. As shown in Fig. 3A, the NO concentration in the + BLM group significantly increased compared to the control group (− BLM), reaching its peak by day 14 post-injury ($p < 0.01$). By day 28, the NO levels returned to normal, coinciding with the resolution phase of the inflammatory reaction. In the group treated with hFL-MSCs (BLM + MSC), the NO production was significantly lower than in the + BLM group during the inflammatory phase (up to day 14).

Lung wet/dry weight ratio assay

As shown in Fig. 3B, the wet/dry (W/D) weight ratio was significantly increased in the + BLM group compared to the control group (− BLM) on days 3 and 7 post-injury, indicating the presence of pulmonary edema. Cell therapy with hFL-MSCs (BLM + MSC) significantly reduced the W/D ratio compared to the + BLM group ($p < 0.05$) at both time points, suggesting a reduction in pulmonary edema. On day 14, the W/D ratio was significantly lower in the BLM + MSC group compared to the + BLM group ($p < 0.05$), demonstrating a prolonged therapeutic effect of the hFL-MSCs. By day 28, no significant differences in the W/D ratio were observed between any of the groups, indicating a resolution of pulmonary edema across all groups.

Histological evaluations

Hematoxylin and Eosin (H&E) staining In histological evaluation (Fig. 4A), the control group (− BLM) showed a normal structure with clear pulmonary alveoli without any exudates or edema at all time points.

In the rats received bleomycin, but did not undergo cell therapy (+ BLM), the typical histopathological features of acute lung injury over a time course extending from post-injury day 3 to 28 were seen. In the + BLM group, a progressive distortion of the lung architecture was observed over time. On post-injury day 3, large numbers of inflammatory cells were present in the interstitial area. Peribronchiolar interstitial pneumonia (rectangles), interstitial granulomatous inflammation (circles), and Langhans giant cells (arrows) were also noted. By day 7, inflammatory reactions were evident in the parenchyma, around blood vessels, and airways (rectangles and circles). Perivascular inflammatory exudate (white arrowhead) and active alveolar macrophages (arrows) were prominent. On day 14, granulomatous reactions (rectangles), fibrotic reactions (arrows), fibroblast proliferation

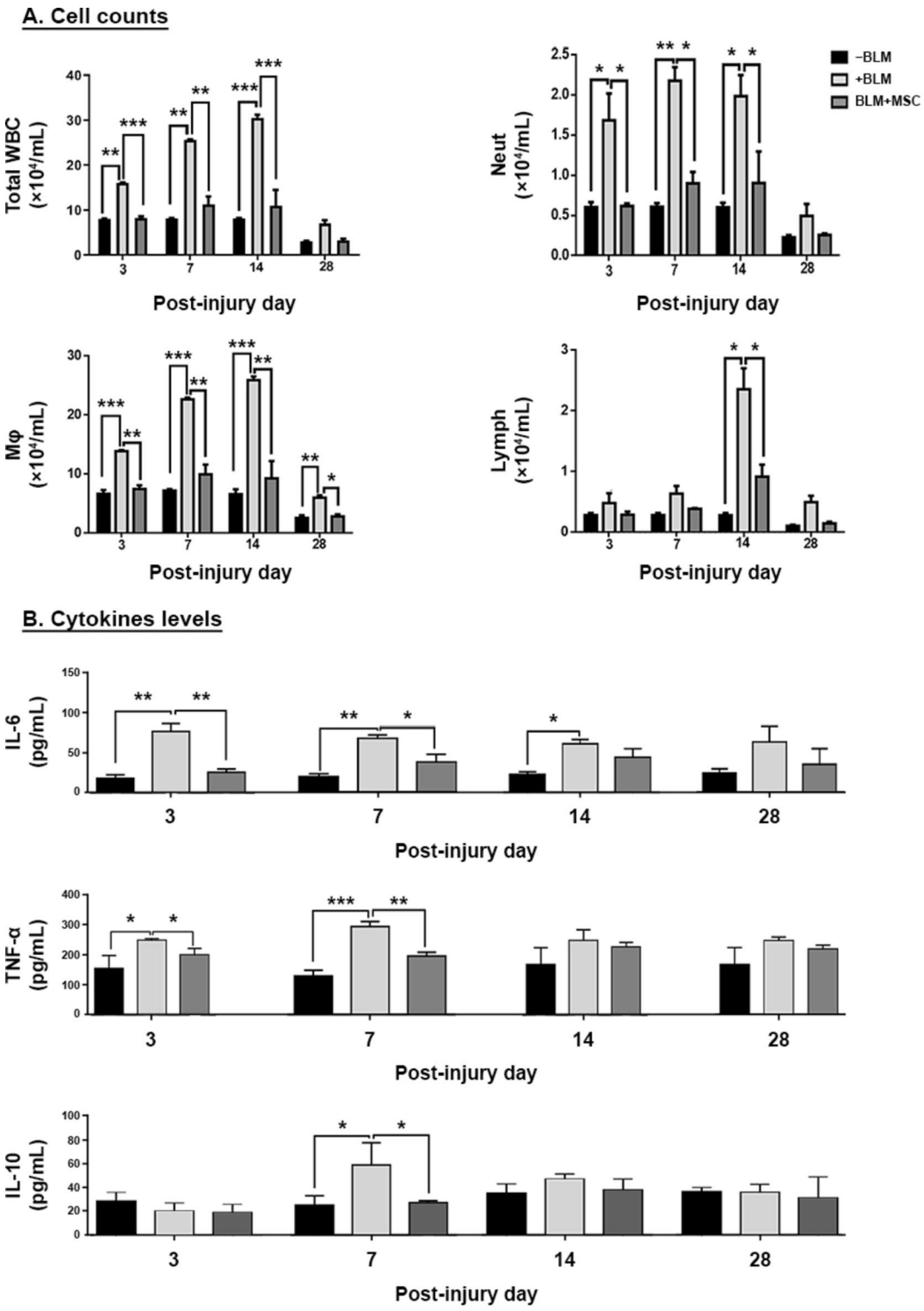

and foci of hemorrhage (circles) were observed. By day 28, notable smooth muscle hypertrophy and hyperplasia (arrows) and obliteration of the vascular lumen (circles) were observed.

In the rats that underwent cell therapy with hFL-MSCs after induction of ALI (BLM + MSC), lung histology showed reduced infiltration of inflammatory cells and less thickening of the lung interstitium compared to the untreated group. Specifically, on post-injury day 3, there was mild interstitial inflammation (rectangles) and extravasated RBCs (arrow). Then, by day 7, mild thickening of the inter-alveolar septa (arrow) and a low number of inflammatory cells in the interstitium (rectangles) were observed. Furthermore, on day 14, mild peribronchiolitis (rectangles) and inflammatory cells mixed with exfoliated epithelium within the lumen of air ducts (arrows) were noted. Finally, by day 28, only minor foci of inter-alveolar thickening (circle) and a few extravasated RBCs (arrow) were present, with the lung structure returning to near-normal histology.

◂**Fig. 2**. Bronchoalveolar lavage fluid cell counts and cytokines levels. (**A**) Cell counts: Total white blood cells, neutrophils, macrophages, and lymphocytes in BALF on days 3, 7, 14, and 28 after acute lung injury and cell therapy. The + BLM group shows significant increases compared to controls (− BLM) at various time points, which are significantly reduced in the BLM + MSC group. (**B**) Cytokine levels: IL-6, TNF-α, and IL-10 levels in BALF on days 3, 7, 14, and 28 after acute lung injury and cell therapy. Pro-inflammatory cytokines are elevated in the + BLM group during the acute phase (IL-6 up to day 14 and TNF-α up to day 7). The anti-inflammatory cytokine IL-10 shows a transient increase on day 7. The BLM + MSC group shows significant reductions in these cytokines at corresponding time points. Abbreviations: BALF, bronchoalveolar lavage fluid; WBC, white blood cells; Neut, neutrophils; Mφ, macrophages; Lymph, lymphocytes; −BLM, the control rats received PBS instead of bleomycin and cell suspension; +BLM, the rats sustained induced ALI with bleomycin that did not undergo cell therapy, received PBS instead of cell suspension; BLM + MSC, the rats sustained ALI with bleomycin that underwent cell therapy with human fetal lung mesenchymal cells at day 0. Data are mean ± SD; $^{*}p < 0.05$, $^{**}p < 0.01$, $^{***}p < 0.001$ (Only statistically significant differences between groups are indicated in the figure).

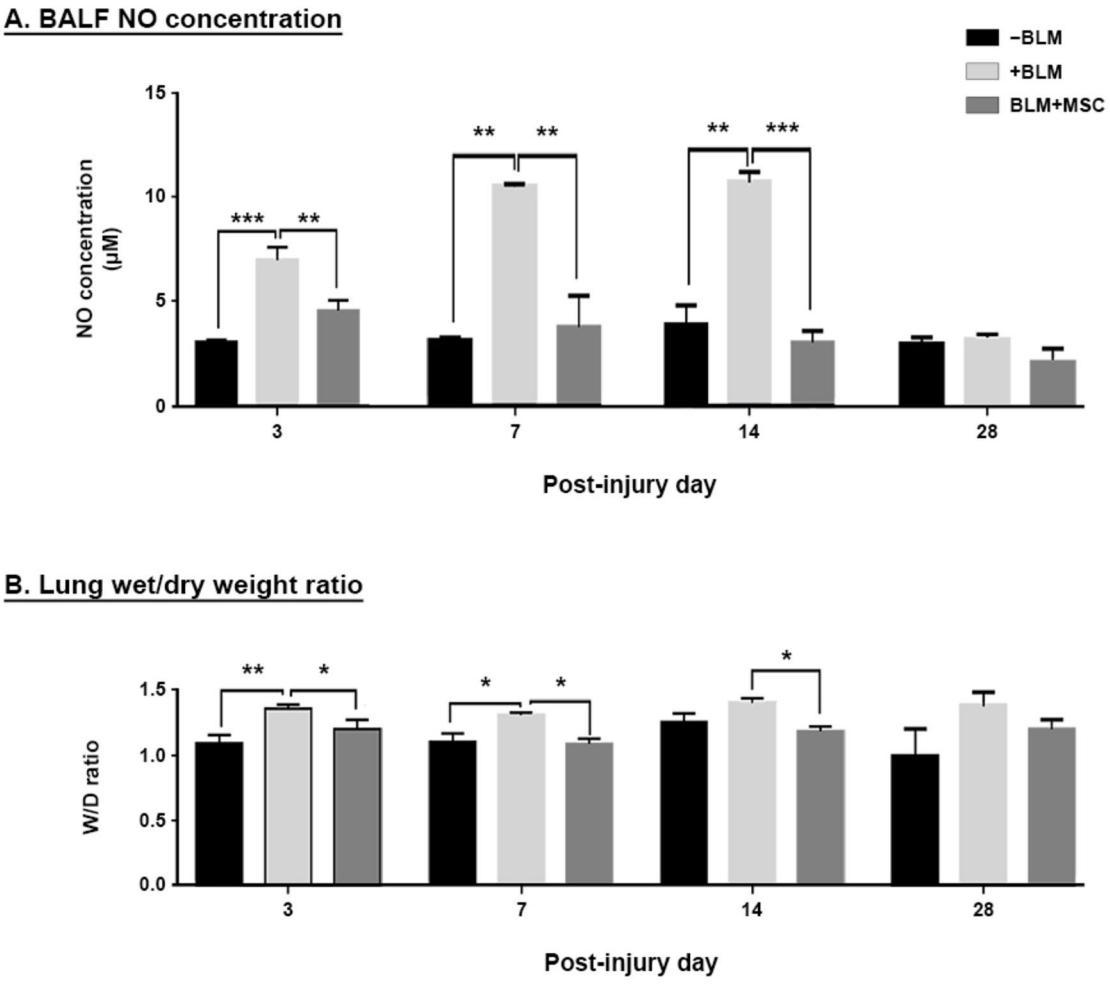

Fig. 3. Bronchoalveolar lavage fluid NO levels and lung edema assessment. (**A**) BALF NO concentration: Levels of nitric oxide were measured in bronchoalveolar lavage fluid on days 3, 7, 14, and 28 after acute lung injury and cell therapy with hFL-MSCs. The + BLM group shows significant increases compared to controls (− BLM) at various time points, which are significantly reduced in the BLM + MSC group. (**B**) Lung wet/dry weight ratio. To evaluate the extent of lung edema, this index was determined on days 3, 7, 14, and 28 after acute lung injury and cell therapy with hFL-MSCs. The + BLM group shows significant accumulation of fluid compared to controls (− BLM) up to day 7. In BLM + MSC group, cell therapy prevented significant fluid accumulation up to day 14. Abbreviations: BALF, bronchoalveolar lavage fluid; NO, nitric oxide; −BLM, the control rats received PBS instead of bleomycin and cell suspension; +BLM, the rats sustained induced ALI with bleomycin that did not undergo cell therapy, received PBS instead of cell suspension; BLM + MSC, the rats sustained ALI with bleomycin that underwent cell therapy with human fetal lung mesenchymal cells at day 0; W/D ratio, wet/dry weight ratio. Data are mean ± SD; $^{*}p < 0.05$, $^{**}p < 0.01$, $^{***}p < 0.001$ (Only statistically significant differences between groups are indicated in the figure).

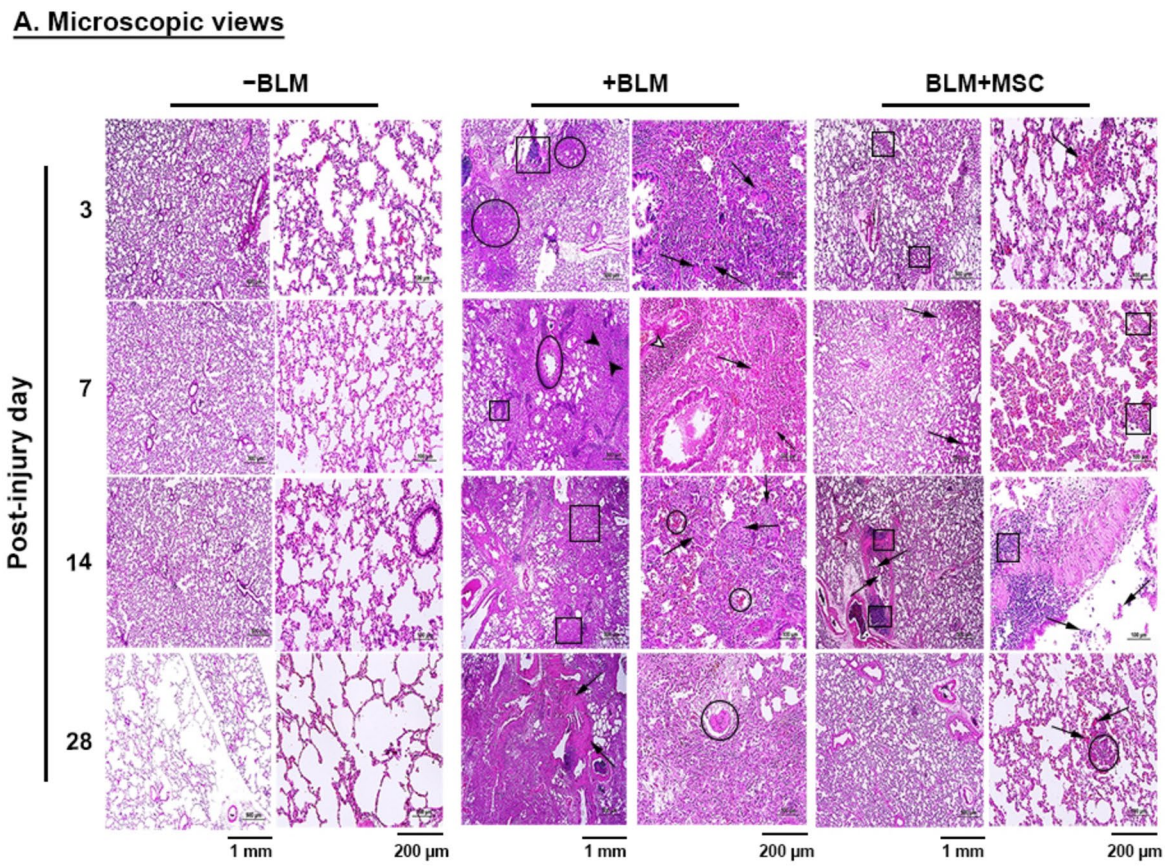

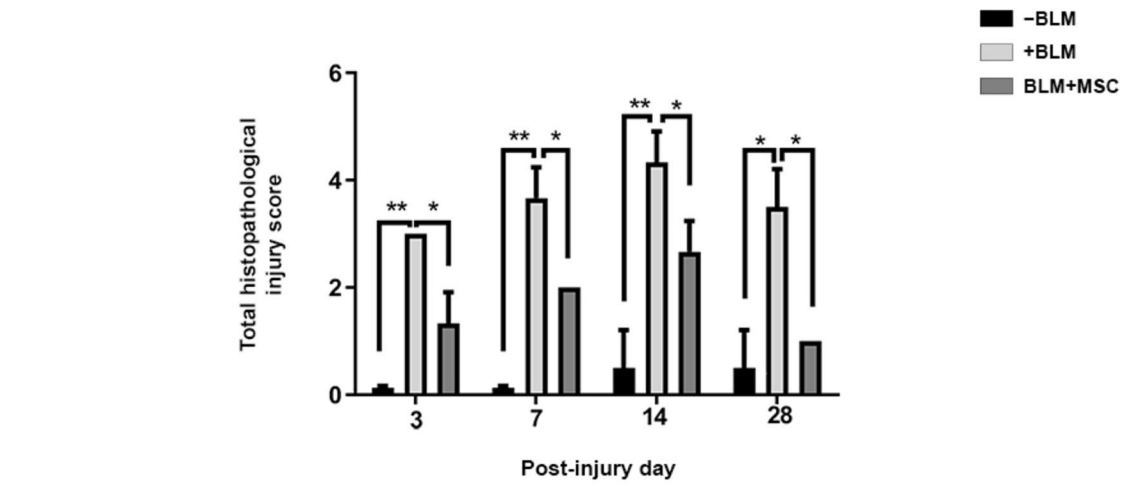

The extent of inflammation in the lungs of each experimental group was semi-quantitatively assessed by the histopathologic scoring presented in the supplementary **Table S2**. The results (Fig. 4B) showed that lung injury scores in + BLM group were significantly higher than the control group (− BLM) at each timepoint. Meanwhile, the injury scores of the group that underwent cell therapy with hFL-MSCs (BLM + MSC) were significantly lower than the + BLM group ($p < 0.05$).

Masson's trichrome staining Masson's trichrome staining was performed to visualize collagen deposition as one of the main indicators of fibrosis (Fig. 5A). BLM administration induced marked collagen deposition and alveolar thickening in lung tissue of + BLM group compared to the animals that did not receive BLM (− BLM). In + BLM group, pulmonary fibrosis, along with progressive deformation of the lung structure, rapidly increased from day 7 to day 28. However, the administration of hFL-MSCs (BLM + MSC group) inhibited collagen deposition and prevented deformation of lung structure as presented in Fig. 5A. Measurement of the relative area with collagen deposition in the lung tissues (Fig. 5B) showed that collagen deposition progressively continued

◀**Fig. 4**. Hematoxylin and Eosin staining. (**A**) Representative lung sections on days 3, 7, 14, and 28 after acute lung injury and cell therapy with human fetal lung mesenchymal stem cells (hFL-MSCs). The control group (− BLM) shows normal structure of lung tissue at all time points. In + BLM group, peribronchiolar interstitial pneumonia (rectangle), interstitial granulomatous inflammation (circle) and Langhans giant cells (arrows) are observed on post-injury day 3; inflammatory reactions in parenchyma (black arrowheads), around vascular structures (rectangle), and airways (circle) as well as perivascular inflammatory exudate (white arrowhead) and active alveolar macrophages (arrows) are observed on post-injury day 7; granulomatous (rectangles) and fibrotic (arrow) reactions as well as hemorrhagic foci (circle) are observed on post-injury day 14; and smooth muscle hypertrophy (arrows) and obliteration of the vascular lumen (circle) are observed on post-injury day 28. In BLM + MSC group, a mild interstitial inflammation (rectangles) and extravasated RBCs (arrow) were observed on post-injury day 3; mild thickening of the inter-alveolar septa (arrow) and low number of inflammatory cells in the interstitium (rectangles) are observed on post-injury day 7; a mild peribronchiolitis (rectangles) and inflammatory cells admixed with exfoliated epithelium within the lumen of air ducts (arrows) are observed on post-injury day 14; minor foci of inter-alveolar thickening (circle) and a few extravasated RBCs (arrow) are observed on post-injury day 28, but, the lung structure shows a return to normal histology on this day. (**B**) Relative comparison of experimental groups for the histopathological injury scores showing decreased scores in the BLM + MSC group compared with + BLM group. Abbreviations: −BLM, the control rats received PBS instead of bleomycin and cell suspension; +BLM, the rats sustained induced ALI with bleomycin that did not undergo cell therapy, received PBS instead of cell suspension; BLM + MSC, the rats sustained ALI with bleomycin that underwent cell therapy with human fetal lung mesenchymal cells at day 0. Data are mean ± SD; $^{*}p < 0.05$, $^{**}p < 0.01$ (Only statistically significant differences between groups are indicated in the figure).

in + BLM group up to day 28 and the deposition was significantly higher than − BLM group. Our interesting finding is that collagen deposition in the controls (− BLM) and the group that received cell therapy after acute lung injury (BLM + MSC) does not differ significantly at any time point.

Real-time RT-PCR

Our results showed that after induction of acute lung injury (+ BLM group), the temporal expression of the genes under study exhibited an initial increase during the inflammatory phase, followed by a decrease during the resolution phase, consistent with the natural progression of ALI compared with the − BLM group (Fig. 6). For the pro-inflammatory genes (Fig. 6A), *Il6* was upregulated early (day 3, $p < 0.01$) in response to injury, peaking within a few days (day 7, $p < 0.001$) and then declining. *Tnf* and *Il1b* were highly upregulated within the first week after injury (day 7, $p < 0.001$) and then declining. The expression pattern of the pro-fibrotic gene *Tgfb1* was as expected as well (Fig. 6B) with an early progressive increase from day 3 ($p < 0.01$) to 7 ($p < 0.001$), a progressive decrease in the second week (but still higher than the − BLM group, $p < 0.05$), and a final decrease to the level of − BLM group on day 28. Finally, the expression of *Col1a1* gene (Fig. 6C) followed the expected timeline for fibrotic response and ECM remodeling after injury. The expression progressively increased from day 7 to 14 (both $p < 0.001$) and then, decreased on day 28.

In the group that underwent cell therapy with hFL-MSCs (BLM + MSC), the expressions of pro-inflammatory and pro-fibrotic genes were modulated and decreased at various time points compared with + BLM group (Fig. 6). As a result, the expression of *Col1a1* gene decreased.

Discussion

This study aimed to explore the regenerating potential of human fetal lung-derived mesenchymal stem cells (hFL-MSCs) in a bleomycin (BLM)-induced mouse model of acute lung injury (ALI). The results demonstrated the ability of hFL-MSCs to modulate inflammatory and fibrotic responses, thereby promoting lung repair and reducing pulmonary fibrosis.

We have isolated mesenchymal cells from the second-trimester human fetal lungs and confirmed their mesenchymal stemness properties by their typical morphology (Fig. 1A), positive expression of the molecular markers CD73, CD90 and CD105, lack of expression of hematopoietic lineage markers CD34 and CD45, and lack of expression of HLA-DR (Fig. 1B). These properties were further validated by functional assays demonstrating differentiation into osteogenic and adipogenic lineages (Fig. 1C).

The cell cycle analysis of hFL-MSCs derived from both 16- and 18-weeks fetuses (Fig. 1D) revealed a low number of cells in the sub-G1 phase, a high number in the G0/G1 phase, and a low to moderate number in both the S and G2/M phases. This indicates a stability in cell cycle distribution and the robustness of these cells for cell therapy applications[27]. Cell cycle analysis suggests that 18-week fetal lung cells initially appear less proliferative (more cells in G0/G1 phase). However, population doubling level (PDL) analysis (Fig. 1D) shows they have significantly higher proliferative capacity over time compared to 16-week fetal lung cells (higher PDL at 72 and 168 h). Thus, 18-week hFL-MSCs were chosen for cell therapy in the animal model.

After bleomycin-induced acute lung injury in rats, analysis of the parameters in the bronchoalveolar lavage fluid (BALF) in the + BLM group (Fig. 2) showed a high neutrophil and macrophage count from day 3 to 14, corresponding to the innate immune response[28]. A high lymphocyte count on day 14 was also observed in + BLM group indicating an adaptive immune response to the antigens released from the damaged cells and tissue[29]. Low numbers of neutrophils and lymphocytes on day 28 in the + BLM group correspond to the subsidence of acute inflammatory and adaptive immune responses. However, higher number of macrophages in this group on day 28 reflects their continued role in promoting healing and resolution, which is characterized by a change in

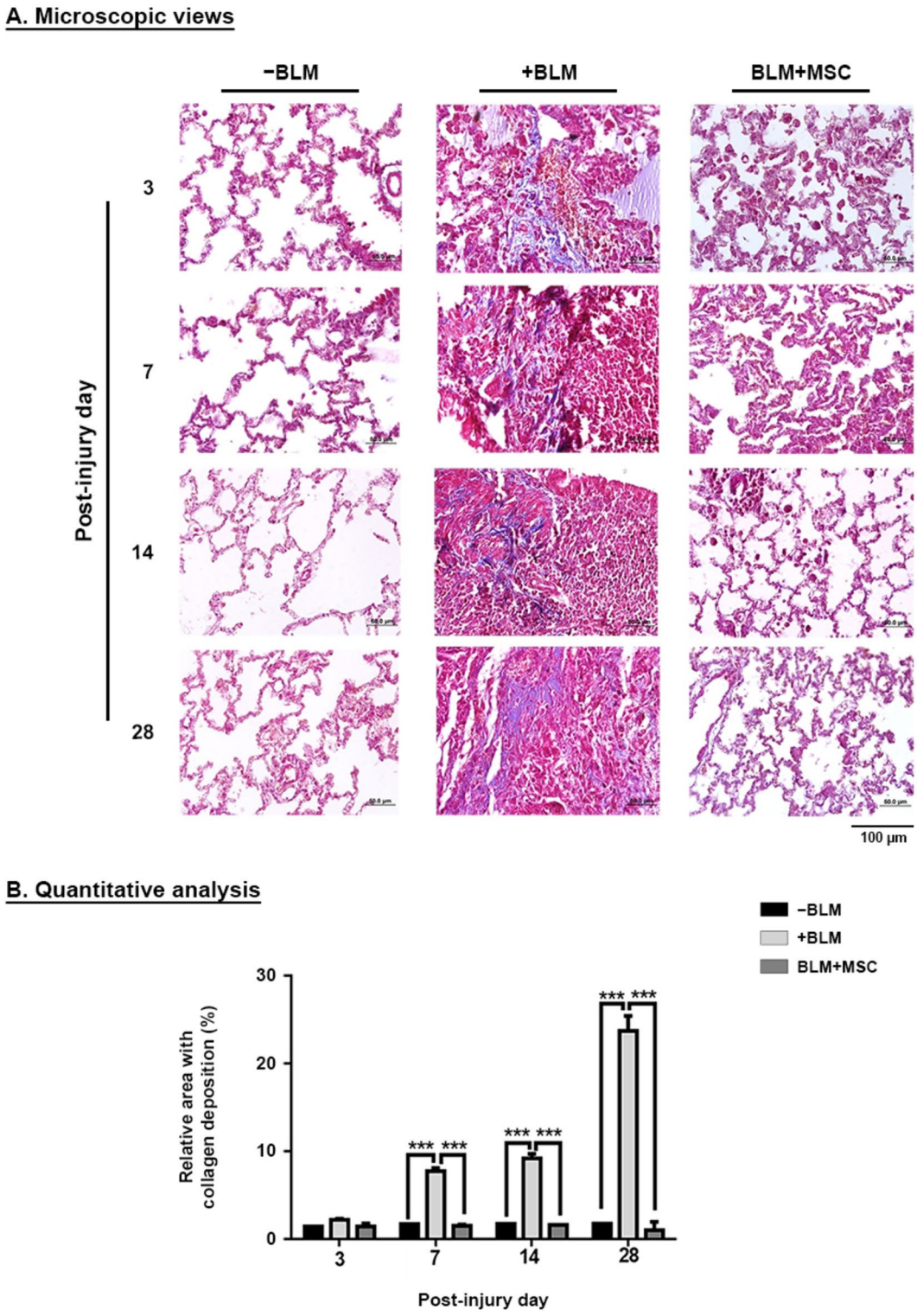

Fig. 5. Masson's trichrome staining. (**A**) Representative lung sections on days 3, 7, 14, and 28 after acute lung injury and cell therapy with human fetal lung mesenchymal stem cells (hFL-MSCs). Collagen fibers are stained blue. In + BLM group dense depositions of collagen and enhanced alveolar thickening are observed. In BLM + MSC group, a noticeable inhibition of collagen deposition in lung tissues is seen. (**B**) Relative comparison of experimental groups for the area with collagen deposition showing decreased deposition in the BLM + MSC group compared with + BLM group. Abbreviations: −BLM, the control rats received PBS instead of bleomycin and cell suspension; +BLM, the rats sustained induced ALI with bleomycin that did not undergo cell therapy, received PBS instead of cell suspension; BLM + MSC, the rats sustained ALI with bleomycin that underwent cell therapy with human fetal lung mesenchymal cells at day 0. Data are mean ± SD; ***$p < 0.001$ (Only statistically significant differences between groups are indicated in the figure).

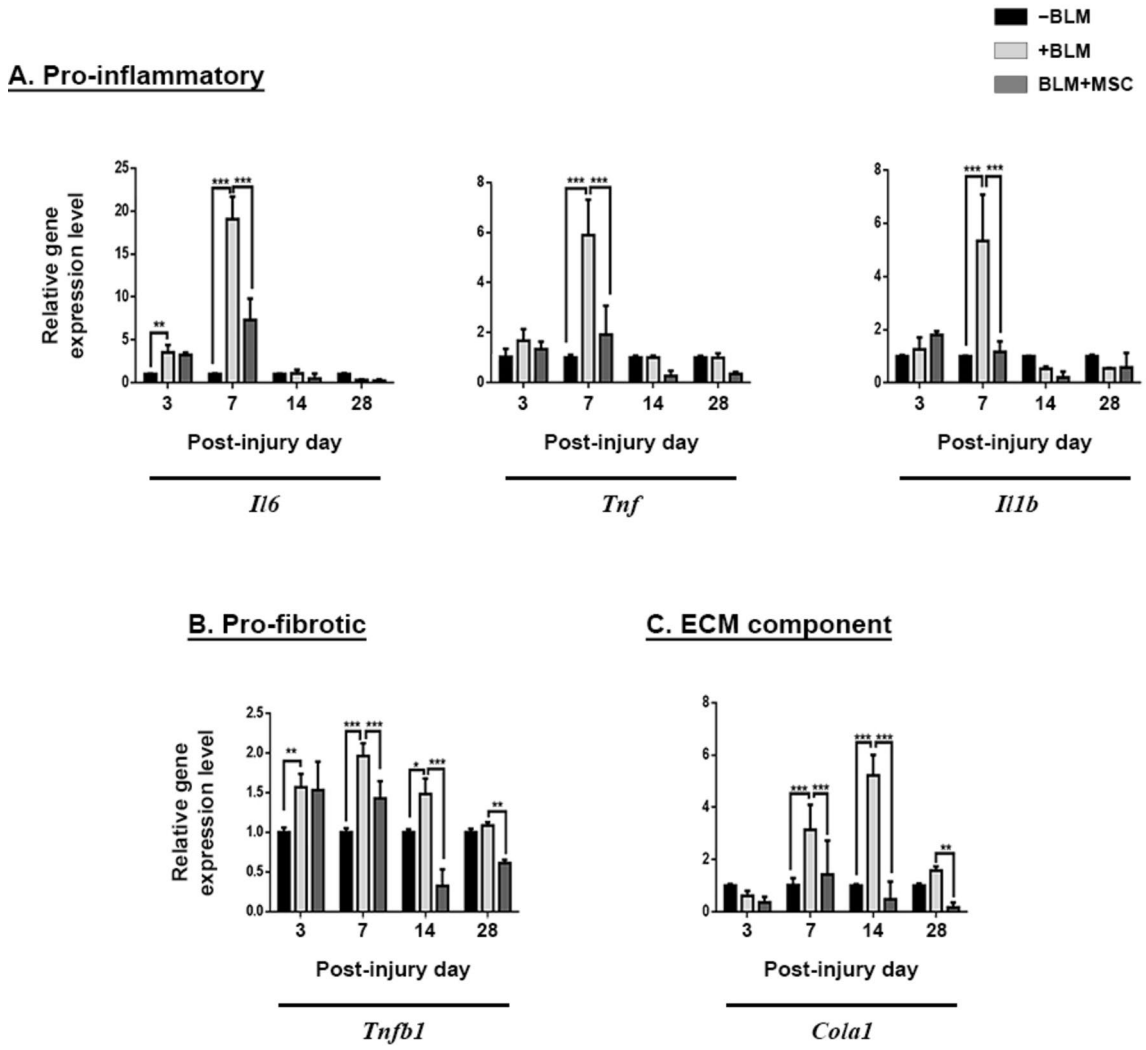

Fig. 6. Gene expression study. Results of real-time RT-PCR on lungs harvested on days 3, 7, 14, and 28 after acute lung injury and cell therapy with human fetal lung mesenchymal stem cells (hFL-MSCs) showing the pattern of expression of (**A**) pro-inflammatory genes, (**B**) pro-fibrotic gene and (**C**) the gene that encodes alpha 1 chain of collagen type I. The temporal expression in + BLM group follows the expected pattern. Cell therapy modulated the expression of the genes in BLM + MSC group. Abbreviations: −BLM, the control rats received PBS instead of bleomycin and cell suspension; +BLM, the rats sustained induced ALI with bleomycin that did not undergo cell therapy, received PBS instead of cell suspension; BLM + MSC, the rats sustained ALI with bleomycin that underwent cell therapy with human fetal lung mesenchymal cells at day 0; ECM, extracellular matrix; *Il6*, interleukin 6; *Tnf*, tumor necrosis factor α; *Il1b*, interleukin 1 beta; *Tgfb1*, transforming growth factor beta 1; *Col1a1*, collagen type I alpha 1 chain; Data are mean ± SD; $^{*}p < 0.05$; $^{**}p < 0.01$; $^{***}p < 0.001$ (Only statistically significant differences between groups are indicated in the figure).

polarization to a reparative phenotype[30]. Our results (Fig. 2A) show that in the BLM + MSC group, the cellular response to acute inflammation and, consequently, to the adaptive immunity was significantly ameliorated by hFL-MSCs.

Our findings show that cytokine levels in the BAL fluid (Fig. 2B) align with immune cell dynamics. In the + BLM group, early increases in IL-6 and TNF-α correlate with acute inflammation driven by neutrophils and macrophages. The rise of IL-10 on day 7 indicates regulatory control of inflammation. By day 28, cytokine levels return to baseline, consistent with inflammation resolution and tissue repair by macrophages. These results align with the previously published report[31]. Consistent with the profile of immune cells, the profile of the cytokines in BLM + MSC group confirms the reduction of the inflammatory response by hFL-MSCs in rat lungs at the time points when the response was increased in + BLM group.

Nitric oxide (NO) concentration in BAL fluid effectively indicates inflammation and treatment effects. During acute lung injury, inflammatory cytokines stimulate NO production in various cells including endothelial and epithelial cells, macrophages, neutrophils, monocytes, and dendritic cells. NO is linked to oxidative stress, potentially causing further lung damage. Also, interaction with superoxide produces peroxynitrite, leading to nitrosative stress[32]. In this study, NO levels in BAL fluid correlated with inflammatory cells and cytokines,

indicating high inflammation and oxidative/nitrosative stress in the + BLM group up to day 14. Cell therapy with hFL-MSCs in the BLM + MSC group effectively reduced this response (Fig. 3A), consistent with the other report[33].

Our findings show that hFL-MSCs significantly reduce pulmonary edema after acute lung injury, as indicated by a lower lung wet/dry (W/D) weight ratio (Fig. 3B). The + BLM group had a high W/D ratio on days 3 and 7, indicating significant edema. In contrast, the BLM + MSC group had a significantly lower W/D ratio at these times, demonstrating the therapeutic efficacy of hFL-MSCs. The reduced W/D ratio on day 14 in the BLM + MSC group suggests prolonged benefits. By day 28, all groups showed resolution of the edema, aligning with other reports on the effectiveness of mesenchymal stem cells in treating ALI[34].

Our histopathological study (Figs. 4 and 5) aligns with BALF analysis and lung W/D ratio changes, showing that hFL-MSCs significantly ameliorate lung injury. H&E staining revealed that the untreated + BLM group had substantial lung architecture distortion, marked by increased inflammatory cell infiltration, interstitial pneumonia, granulomatous inflammation, and fibrosis over 28 days. In contrast, the BLM + MSC group showed reduced inflammation, less interstitial thickening, and minimal fibrosis, indicating effective lung injury mitigation and tissue repair. Semiquantitative histopathological scores were significantly lower in the BLM + MSC group, reinforcing hFL-MSCs' protective effect. Masson's trichrome staining confirmed reduced fibrosis, with the BLM + MSC group showing lower collagen levels. These findings highlight hFL-MSCs' therapeutic potential in managing ALI and preventing long-term fibrosis. Similar results were reported using mesenchymal stem cells from other sources such as bone marrow[35], adipose tissue[36] or Wharton's jelly[37].

Our gene expression study (Fig. 6) indicated that hFL-MSCs modulated key inflammatory and fibrotic gene expression post-ALI. In comparison to the + BLM group, the BLM + MSC group exhibited a significant reduction in the expression of pro-inflammatory genes (*Il6*, *Tnf*, *Il1b*), pro-fibrotic genes (*Tgfb1*) and *Col1a1* gene at various time points. The observed decrease in *Tgfb1* expression by day 28 aligns with its established role as a pro-fibrotic factor, reflecting the resolution of fibrotic processes post-cell therapy. It is important to distinguish this TGF-β isoform from TGF-β3, which is associated with regenerative and anti-fibrotic effects during repair phases[38,39]. Expression of *Tgfb3* gene has not been evaluated in the current study. These findings suggest that hFL-MSCs play a critical role in attenuating both the inflammatory response and fibrotic processes post-injury. These results are consistent with other studies utilizing mesenchymal stem cells (MSCs) from other sources[36,37,40]. Similar to our findings, these studies have reported that MSCs can significantly downregulate pro-inflammatory cytokines and reduce the expression of fibrotic markers in models of lung injury.

Overall, our findings in untreated bleomycin-induced ALI models align with previous studies demonstrating that inflammatory and pro-fibrotic markers peak during the inflammatory phase up to day 14 and decrease in the resolution phase (day 14 onward), reflecting the natural healing process of untreated animals[41–43]. We have shown that this natural temporal dynamic can be modulated by cell therapy with hFL-MSCs. Based on our data and previously reports, the effects of hFL-MSCs could be mainly attributed to the immunomodulatory[15], anti-inflammatory[13] and anti-fibrotic[14] properties of mesenchymal stem cells. Additionally, the fetal origin of the cells results in high plasticity, proliferative capacity[18], and low immunogenicity[44], which are critical for allogenic cell therapy applications.

When considering cell therapy with stem cells, it is important to take into account the observations that these cells retain a memory of their tissue of origin[19,45], and hence, have a tissue-specific preference for homing and regenerating capacity. This can help in designing more efficient regenerative therapy protocols and represents the novelty of the current study. Based on this concept, fetal stem cells have been sucessfully used for tissue-specific injury repair in some studies. For example, fetal liver and neural stem cells were used for the treatment of liver injury[46] and Alzheimer's type neurodegeneration[47] in animal models. Moreover, in our previous study, we demonstrated that in a rat model of lung injury, cell therapy with human fetal respiratory epithelial cells, including epithelial stem cells, significantly improves the process and outcome of tissue healing in the lungs[24].

Based on our proof-of-concept studies with fetal respiratory epithelial and mesenchymal cells, it can be suggested that one of the potentially viable sources of cells for therapy of lung injuries is the cells with the phenotypic and functional characteristics of fetal respiratory stem cells, including epithelial and mesenchymal cells. Therefore, if pluripotent cells, such as iPS cells, are considered as the source for cell therapy in respiratory conditions, their pre-differentiation into fetal respiratory epithelial and mesenchymal stem cell phenotype should be considered. The novelty of this study lies in introducing this concept, which leverages the unique properties of fetal lung-derived cells, represents a significant step forward in the quest to develop specific, targeted treatments for this challenging condition.

Conclusion

This study shows that hFL-MSCs promote lung repair and reduce fibrosis and edema in a bleomycin-induced ALI model. Our results highlight the benefits of using fetal stem cells, particularly those with respiratory phenotypes, for treating lung injuries. Based on this report, future therapies could explore pre-differentiating stem cells, including pluripotent stem cells, into fetal respiratory mesenchymal stem cell phenotypes. This approach leverages the tissue-specific regenerative capabilities observed in fetal respiratory cells, potentially enhancing the efficacy and specificity of cell therapy for respiratory conditions.

Data availability

The raw data supporting the conclusions of this article will be made available by the authors upon reasonable request to the corresponding author.

Received: 31 August 2024; Accepted: 20 February 2025

Published online: 21 February 2025

References

1. Grotberg, J. C., Reynolds, D. & Kraft, B. D. Management of severe acute respiratory distress syndrome: a primer. *Crit. Care*. **27** (1), 289 (2023).
2. Chioccioli, M. et al. Stem cell migration drives lung repair in living mice. *Dev. Cell.* **59** (7), 830–840e4 (2024).
3. Serrano-Mollar, A. et al. Intratracheal transplantation of alveolar type II cells reverses bleomycin-induced lung fibrosis. *Am. J. Respir Crit. Care Med.* **176** (12), 1261–1268 (2007).
4. Siti-Ismail, N. et al. Development of a novel three-dimensional, automatable and integrated bioprocess for the differentiation of embryonic stem cells into pulmonary alveolar cells in a rotating vessel bioreactor system. *Tissue Eng. Part. C Methods*. **18** (4), 263–272 (2012).
5. Ma, N. et al. Mesenchymal stem Cell-derived type II alveolar epithelial progenitor cells attenuate LPS-induced acute lung injury and reduce P63 expression. *Curr. Stem Cell. Res. Ther.* **19** (2), 245–256 (2024).
6. Alvarez-Palomo, B. et al. Induced pluripotent stem cell-derived lung alveolar epithelial type II cells reduce damage in bleomycin-induced lung fibrosis. *Stem Cell. Res. Ther.* **11** (1), 213 (2020).
7. Guillamat-Prats, R. et al. *Alveolar type II cells or mesenchymal stem cells: comparison of two different cell therapies for the treatment of acute lung injury in rats*. *Cells*, **9**(8). (2020).
8. Feng, Y. & Wang, B. Automated closed-cell production platform solves dilemma of industrial-scale manufacturing for mesenchymal stromal cell-based therapy. *J. Pharm. Anal.* **13** (11), 1233–1234 (2023).
9. Strecanska, M. et al. *Automated Manufacturing Processes and Platforms for large-scale Production of clinical-grade Mesenchymal Stem/ Stromal Cells* (Stem Cell Reviews and Reports, 2024).
10. Liang, J. et al. Recent progress in mesenchymal stem cell-based therapy for acute lung injury. *Cell. Tissue Bank.* **25** (2), 677–684 (2024).
11. Rolandsson Enes, S. & Weiss, D. J. Cell therapy for lung disease: current status and future prospects. *Curr. Stem Cell Rep.* **6** (2), 30–39 (2020).
12. Xu, X. et al. Comparative effects of umbilical cord mesenchymal stem cell treatment via different routes on Lipopolysaccharide-Induced acute lung injury. *Front. Biosci. (Landmark Ed)*. **29** (6), 217 (2024).
13. Huh, J. W. et al. Anti-inflammatory role of mesenchymal stem cells in an acute lung injury mouse model. *Acute Crit. Care*. **33** (3), 154–161 (2018).
14. Harrell, C. R. et al. *Molecular mechanisms responsible for the therapeutic potential of mesenchymal stem Cell-Derived exosomes in the treatment of lung fibrosis*. *Int. J. Mol. Sci.*, **25**(8). (2024).
15. Li, J. P. et al. *Immunomodulation of mesenchymal stem cells in acute lung injury: from preclinical animal models to treatment of severe COVID-19*. *Int. J. Mol. Sci.*, **23**(15). (2022).
16. Zhong, Y. et al. Human embryonic stem cell-derived mesenchymal stromal cells suppress inflammation in mouse models of rheumatoid arthritis and lung fibrosis by regulating T-cell function. *Cytotherapy*, (2024).
17. Rolandsson Enes, S. et al. MSC from fetal and adult lungs possess lung-specific properties compared to bone marrow-derived MSC. *Sci. Rep.* **6**, 29160 (2016).
18. Gençer, E. B. et al. Transcriptomic and proteomic profiles of fetal versus adult mesenchymal stromal cells and mesenchymal stromal cell-derived extracellular vesicles. *Stem Cell. Res. Ther.* **15** (1), 77 (2024).
19. Andrzejewska, A., Lukomska, B. & Janowski, M. Concise review: mesenchymal stem cells: from roots to boost. *Stem Cells*. **37** (7), 855–864 (2019).
20. Wang, C. et al. In vivo tracking of mesenchymal stem cell dynamics and therapeutics in LPS-induced acute lung injury models. *Exp. Cell. Res.* **437** (2), 114013 (2024).
21. Wang, L. et al. Biomimetic scaffold-based stem cell transplantation promotes lung regeneration. *Bioeng. Transl Med.* **8** (4), e10535 (2023).
22. Samadikuchaksaraei, A. et al. Derivation of distal airway epithelium from human embryonic stem cells. *Tissue Eng.* **12** (4), 867–875 (2006).
23. Samadikuchaksaraei, A. & Bishop, A. E. Effects of growth factors on the differentiation of murine ESC into type II pneumocytes. *Cloning Stem Cells*. **9** (3), 407–416 (2007).
24. Ganji, F. et al. Epithelial cells/progenitor cells in developing human lower respiratory tract: characterization and transplantation to rat model of pulmonary injury. *Bioimpacts* **13** (6), 505–520 (2023).
25. Jahromi, G. P. et al. Characterization of lung fibroblasts more than two decades after mustard gas exposure. *PloS One*. **10** (12), e0145148 (2015).
26. Shirani, A. et al. Cross-linked acellular lung for application in tissue engineering: effects on biocompatibility, mechanical properties and immunological responses. *Mater. Sci. Eng. C Mater. Biol. Appl.* **122**, 111938 (2021).
27. Zhao, H., Zhao, H. & Ji, S. *A Mesenchymal Stem Cell Aging Framework, from Mechanisms To Strategies* (Stem Cell Rev Rep, 2024).
28. Matute-Bello, G., Frevert, C. W. & Martin, T. R. Animal models of acute lung injury. *Am. J. Physiol. Lung Cell. Mol. Physiol.* **295** (3), L379–L399 (2008).
29. Izbicki, G. et al. Time course of bleomycin-induced lung fibrosis. *Int. J. Exp. Pathol.* **83** (3), 111–119 (2002).
30. Malainou, C. et al. *Alveolar macrophages in tissue homeostasis, inflammation, and infection: evolving concepts of therapeutic targeting.* J Clin Invest, 133(19). (2023).
31. Noguchi, S. et al. Nitric oxide exerts protective effects against bleomycin-induced pulmonary fibrosis in mice. *Respir Res.* **15** (1), 92 (2014).
32. Bezerra, F. S. et al. *Oxidative stress and inflammation in acute and chronic lung injuries*. *Antioxid. (Basel)*, **12**(3). (2023).
33. Lv, H. et al. Heat shock preconditioning mesenchymal stem cells attenuate acute lung injury via reducing NLRP3 inflammasome activation in macrophages. *Stem Cell. Res. Ther.* **12** (1), 290 (2021).
34. Gupta, N. et al. Intrapulmonary delivery of bone marrow-derived mesenchymal stem cells improves survival and attenuates endotoxin-induced acute lung injury in mice. *J. Immunol.* **179** (3), 1855–1863 (2007).
35. Zhang, E. et al. Efficacy of bone marrow mesenchymal stem cell transplantation in animal models of pulmonary fibrosis after exposure to bleomycin: A meta-analysis. *Exp. Ther. Med.* **17** (3), 2247–2255 (2019).
36. Llontop, P. et al. Airway transplantation of adipose stem cells protects against bleomycin-induced pulmonary fibrosis. *J. Investig Med.* **66** (4), 739–746 (2018).
37. Zhu, H. et al. Therapeutic effects of human umbilical Cord-Derived mesenchymal stem cells in acute lung injury mice. *Sci. Rep.* **7**, 39889 (2017).
38. Lichtman, M. K., Otero-Vinas, M. & Falanga, V. Transforming growth factor beta (TGF-β) isoforms in wound healing and fibrosis. *Wound Repair. Regeneration*. **24** (2), 215–222 (2016).
39. Samadikuchaksaraei, A. et al. A dermal equivalent engineered with TGF-β3 expressing bone marrow stromal cells and amniotic membrane: cosmetic healing of Full-Thickness skin wounds in rats. *Artif. Organs*. **40** (12), E266–E279 (2016).
40. Zhao, Y. et al. Effectivity of mesenchymal stem cells for bleomycin-induced pulmonary fibrosis: a systematic review and implication for clinical application. *Stem Cell. Res. Ther.* **12** (1), 470 (2021).

41. Mahmutovic Persson, I. et al. Imaging biomarkers and Pathobiological profiling in a rat model of Drug-Induced interstitial lung disease induced by bleomycin. *Front. Physiol.* **11**, 584 (2020).
42. Ruscitti, F. et al. Longitudinal assessment of bleomycin-induced lung fibrosis by Micro-CT correlates with histological evaluation in mice. *Multidisciplinary Respiratory Med.* **12**, 8 (2017).
43. Kim, B. M. et al. *Gas6 ameliorates inflammatory response and apoptosis in Bleomycin-Induced acute lung injury*. *Biomedicines*, **9**(11). (2021).
44. Chen, P. M. et al. Immunomodulatory properties of human adult and fetal multipotent mesenchymal stem cells. *J. Biomed. Sci.* **18** (1), 49 (2011).
45. Ng, T. T. et al. *Murine mesenchymal stromal cells retain biased differentiation plasticity towards their tissue of origin*. *Cells*, **9**(3). (2020).
46. Irudayaswamy, A. et al. Long-Term fate of human fetal liver progenitor cells transplanted in injured mouse livers. *Stem Cells*. **36** (1), 103–113 (2018).
47. Poltavtseva, R. A. et al. Effect of transplantation of neural stem and progenitor cells on memory in animals with Alzheimer's type neurodegeneration. *Bull. Exp. Biol. Med.* **168** (4), 589–596 (2020).

Acknowledgements

We would like to express our sincere gratitude to Dr. Hannaneh Golshahi from the Avicenna Research Institute, Tehran, Iran, for her invaluable contributions to this research. Her expertise and dedication in performing the pathological analyses were crucial to the success of this study. Also, we would like to thank Iran University of Medical Sciences (IUMS), Tehran, Iran for its full support of this project and specifically Shahid Akbarabadi Clinical Research Development Unit (shACRDU) for providing fetal samples. Additionally, we extend our thanks to Shahid Sadoughi University of Medical Sciences, Yazd, Iran, for its support and collaboration in facilitating the research process. The authors acknowledge the use of several AI tools including ChatGPT, Copilot, and Perplexity for assistance with language editing to enhance the clarity and fluency of the manuscript. The authors take full responsibility for the content and conclusions of this work.

Author contributions

Mahtab Golmohammadi: Methodology; Investigation; Data curation; Formal analysis; Visualization; Writing–original draft; Writing–review & editing. Mohammad Hasan Sheikhha: Writing–review & editing. Fatemeh Ganji: Methodology; Investigation; Writing–review & editing. Ali Shirani: Methodology; Investigation; Writing–review & editing. Mahmood Barati: Methodology; Writing–review & editing. Seyed Mehdi Kalantar: Methodology; Writing–review & editing. Seyed Mohammad Amin Haramshahi: Methodology; Writing–review & editing. Nushin Karkuki Osguei: Writing–review & editing. Ali Samadikuchaksaraei: Conceptualization; Funding acquisition; Project administration; Supervision; Resources; Methodology; Software; Formal analysis; Visualization; Validation; Writing–original draft; Writing–review & editing.

Funding

This work was supported by grants from the Iran University of Medical Sciences (98-04-14-16074) and the Iranian Council for Development of Stem Cell Sciences and Technologies (11/79319).

Declarations

Competing interests

Samadikuchaksaraei is shareholder and CEO of Baztarmim Company, which is focused on production of tissue engineering products. Other authors have no conflicts of interest to declare.

Ethics

The study was approved by the Ethical Committees of the Iranian Ministry of Health (code: EC-00264, 17 August 2013), the Iran University of Medical Sciences (IUMS) (code: IR.IUMS.rec.1393.25093, 30 September 2014) and Iranian Academic Center for Education, Culture and Research (code: IR.ACERE.ROYAN.REC.1398.186, 28 October 2019). All fetuses were obtained with written informed consent.

Additional information

Supplementary Information The online version contains supplementary material available at https://doi.org/10.1038/s41598-025-91406-0.

Correspondence and requests for materials should be addressed to A.S.